Journal of Cerebral Blood Flow & Metabolism (2013) 33, 1725–1731

www.jcbfm.com

ORIGINAL ARTICLE

Reference region automatic extraction in dynamic [^{11}C]PIB

Yoko Ikoma[1], Paul Edison[2], Anil Ramlackhansingh[2], David J Brooks[2] and Federico E Turkheimer[2,3]

The positron emission tomography (PET) radiotracer [^{11}C]Pittsburgh Compound B (PIB) is a marker of amyloid plaque deposition in brain, and binding potential is usually quantified using the cerebellum as a reference where the specific binding is negligible. The use of the cerebellum as a reference, however, has been questioned by the reported cerebellar [^{11}C]PIB retention in familial Alzheimer's disease (AD) subjects. In this work, we developed a supervised clustering procedure for the automatic extraction of a reference region in [^{11}C]PIB studies. Supervised clustering models each gray matter voxel as the linear combination of three predefined kinetic classes, normal and lesion gray matter, and blood pool, and extract reference voxels in which the contribution of the normal gray matter class is high. In the validation with idiopathic AD subjects, supervised clustering extracted reference voxels mostly in the cerebellum that indicated little specific [^{11}C]PIB binding, and total distribution volumes of the extracted region were lower than those of the cerebellum. Next, the methodology was applied to the familial AD cohort where the cerebellar amyloid load had been demonstrated previously, resulting in higher binding potential compared with that obtained with the cerebellar reference. The supervised clustering method is a useful tool for the accurate quantification of [^{11}C]PIB studies.

Journal of Cerebral Blood Flow & Metabolism (2013) **33,** 1725–1731; doi:10.1038/jcbfm.2013.133; published online 7 August 2013

Keywords: [^{11}C]PIB; PET; reference region; supervised clustering

INTRODUCTION

Positron emission tomography (PET) with [^{11}C]Pittsburgh Compound B (PIB) has been utilized for the *in vivo* imaging of amyloid plaque deposition in the human brain, and has consistently demonstrated a robust amyloid load in Alzheimer's disease (AD) patients when compared with age-matched controls.[1–3] Initially, compartmental and graphical kinetic techniques have been used for the quantification of the tracer binding with an arterial input function.[4] Subsequently, simpler kinetic methods with a reference input have been adopted and, using the cerebellum as a reference, have demonstrated effective quantification ability to retain the discriminatory power between AD and matched controls.[5] Reference region methodologies have obvious appeal for clinical use because they do not require arterial blood sampling, which is logistically challenging, more so in elderly or impaired subjects. Recently, however, [^{11}C]PIB retention in the cerebellum was reported in presenilin 1 mutation carriers compared with normal volunteers,[6,7] suggesting that this region may not be generally suitable as a reference region. Anatomic references other than the cerebellum can be sought, such as the pons as we previously showed.[8] However, there is now a growing interest in an automatic procedure that is able to identify accurately a reference region for [^{11}C]PIB dynamic studies. Although the target-to-reference signal in AD is quite large, research focus is now shifting toward disease progression and toward subjects with low or mild uptake;[9,10] in this context, small specific uptake in the reference may hamper the required accuracy in quantification. Second, novel application of [^{11}C]PIB as a myelin marker and its application to neurodegenerative disorders such as multiple sclerosis,[11] reflects an obvious need for an automatic reference tissue methodology that may depart from the *a priori* definition of an anatomic region given the high uncertainty in the spatial pattern that is targeted.

Automatic clustering was first proposed to extract the reference region for brain PET studies in which the anatomic definition of a region without specific binding was difficult, for example, in the case of the neuroinflammatory marker [^{11}C]-(R)-PK11195 given its unpredictable distribution pattern.[12] In this context, the automatic method segmented brain voxels into classes on the basis of their time–activity courses and selected as reference the class of voxels that exhibited the kinetic behavior closer to that of gray matter in healthy controls. The approach was subsequently refined to increase the reliability of reference extraction for [^{11}C]-(R)-PK11195 study using a supervised approach, that modeled each pixel's time–activity curve (TAC) as the sum of six predefined kinetic classes, normal gray matter, white matter, pathologic peripheral benzodiazepine receptor binding, vascular binding, muscle, and the skull.[13] Multi-center validation of the approach has further confirmed that supervised reference region extraction is indeed the optimal reference approach for [^{11}C]-(R)-PK11195 quantification.[14]

In the present study, we optimized the supervised procedure for the extraction of a reference region in [^{11}C]PIB PET studies, and validated this method in the [^{11}C]PIB studies of idiopathic AD subjects where a plasma input function was available. In particular, we wished to demonstrate that in these AD subjects, the algorithm was able to select reference voxels that lacked a specific-binding component that was identified through the plasma input. The method was then applied to a cohort of familial AD patients where the cerebellar uptake had been previously demonstrated.

[1]Biophysics Group, Molecular Imaging Center, National Institute of Radiological Sciences, Chiba, Japan; [2]Division of Brain Sciences, Hammersmith Hospital, Imperial College London, London, UK and [3]Centre for Neuroimaging, Institute of Psychiatry, King's College London, London, UK. Correspondence: Dr FE Turkheimer, Centre for Neuroimaging, Institute of Psychiatry, King's College London, P089, De Crespigny Park, London SE5 8AF, UK.
E-mail: federico.turkheimer@kcl.ac.uk
FET was supported by the 'PET Methodology Programme Grant' from the Medical Research Council UK (G1100809/1).
Received 24 January 2013; revised 16 June 2013; accepted 10 July 2013; published online 7 August 2013

MATERIALS AND METHODS

Algorithm Implementation of Supervised Clustering for [11C]PIB

The supervised clustering approach for [11C]PIB PET study (Super-PIB) was constructed as an extension of the one developed for [11C]PK11195.[13] This algorithm consists of three elements: (1) an input normalization procedure to scale each frame of the dynamic sequence, (2) a set of predefined kinetic classes, (3) a regression procedure to calculate the contribution of each kinetic class to the signal of each voxel. These weights, and in particular those of the gray matter class, are then used to calculate the reference input TAC.

Normalization of positron emission tomography dynamic sequence. In the PET dynamic images, the radioactivity of each frame was normalized for every voxels in the brain by subtracting the mean frame activity and dividing it by the frame standard deviation (SD) to create a unit input.

$$P_i^n(t) = \frac{P_i(t) - P_{\text{mean}}(t)}{P_{\text{sd}}(t)} \quad (1)$$

where P_i is the radioactivity concentration of i'th voxel, P_{mean} and P_{sd} are the mean and SD of radioactivity concentration for all voxels within the gray matter and white matter, respectively.

Predefined kinetic classes. Three kinetic classes of normal gray matter (class 1), high specific-binding gray matter (class 2), and blood pool (class 3), were predefined from the normalized PET dynamic sequence. The kinetic class of normal gray matter was extracted from the average of normalized time course (P_i^n) in the gray matter for 8 control subjects. The gray matter was identified using coregistered structural scans. For each subject, gray matter was defined from voxels in which the value of gray matter map was higher than 90% of the maximum value. Meanwhile, the kinetic class of high specific-binding gray matter was obtained from the average of normalized time course for three AD subjects sampled on the prefrontal cortex that has been consistently reported to demonstrate substantial specific [11C]PIB retention in AD.[4] Finally, the kinetic class of blood pool was defined from eight control subjects by extracting 30 voxels in which the radioactivity concentration of initial 60 seconds was the highest among all voxels in the brain. The definition of this class aims at avoiding voxels, particularly in the cerebellum, that are too close to venous sinuses and therefore are not representative of normal gray matter.

Estimation of each class contribution. The supervised clustering algorithm modeled the normalized kinetic of voxel i in the gray matter of PET dynamic sequence, identified via the structural MR scan, as a weighted linear combination of the predefined kinetic classes as follows;

$$P_i^n(t) = w_{i1}K_1^n(t) + w_{i2}K_2^n(t) + w_{i3}K_3^n(t) \quad (w_{i1}, w_{i2}, w_{i3} \geq 0) \quad (2)$$

where K_1^n, K_2^n, K_3^n are the predefined kinetic of class 1, 2, and 3, respectively.

The weights w_1, w_2, w_3 were calculated for each voxel within the gray matter by solving equation (2) with the nonnegative least-squares algorithm.[15] In addition, weight ratios were calculated as follows;

$$R_{ik} = w_{ik}/(w_{i1} + w_{i2} + w_{i3}) \quad (k = 1, 2, 3) \quad (3)$$

Extraction of reference region. Voxels in which the ratio of class 1 (R_1) was higher than 0.9 were regarded as the reference region, and the TAC of reference region $C_r(t)$ was finally calculated from these voxels as a weighted average of the non-normalized voxel TAC as;

$$C_r(t) = \sum_{i=1}^{N} w_{i1}P_i(t) \Big/ \sum_{i=1}^{N} w_{i1} \quad (4)$$

where N is the number of voxels regarded as the reference region.

Note that the threshold value of $R_1 = 0.9$ is a good compromise to obtain highly homogeneous gray matter in a large enough number of voxels.

Positron Emission Tomography Study

Eight healthy control subjects, 10 patients with idiopathic AD, and eight patients with familial AD (presenilin 1 mutation carriers AD) participated in this study. Patient data have been reported in the previously published investigation.[7] Elevated [11C]PIB binding was reported in some elderly normal volunteers,[16–20] but this was not the case in healthy control subjects enrolled in this study. Ethical approval was granted by the Hammersmith Hospitals Trust Ethics Committee, and permission to administer radioisotopes was granted by the Administration of Radioactive Substances Advisory Committee of the Department of Health, UK. Informed written consent was obtained from all patients and healthy volunteers. All scans were performed in accordance with the guideline of Hammersmith Hospitals Trust Ethics Committee.

PET studies with [11C]PIB were performed on an ECAT EXACT HR+ (CTI/Siemens) PET camera with 15.5-cm axial field of view, 63 transaxial planes. A transmission scan was acquired before an emission scan using a single rotating photon point source of 150 MBq of ^{137}Cs for subsequent attenuation correction and scatter correction. ~370 MBq of [11C]PIB was administered by a bolus injection 30 seconds after the start of emission scan. The specific radioactivity was 20,235 (±6240) MBq/μmol at the time of injection. Emission data were then acquired over 90 minutes in list mode and reorganized as 32 time frames (30-s background frame, 1 × 15-s frame, 1 × 5-s frame, 1 × 10-s frame, 2 × 30-s frames, 9 × 60-s frames, 3 × 180-s frames, and 14 × 300-s frames). The data were reconstructed by a filtered back-projection using ramp filter set at 0.5 times the Nyquist frequency. The transaxial and axial spatial resolution of the reconstructed images were 5.6 and 5.4 mm full width at half maximum, respectively, at 10-cm distance from the center.

Arterial blood sampling was carried out for healthy controls and idiopathic AD subjects, not for the familial AD subjects, because it was not possible to obtain consent for this particular cohort. Arterial whole blood activity was monitored continuously for the first 15 minutes of the scan with a bismuth germinate coincidence detector at a flow rate of 5 mL/minute. At the same time, discrete arterial blood samples were withdrawn at 5, 10, 15, 20, 30, 40, 50, 60, 75, and 90 minutes after the injection into heparinized syringes, and the radioactivity concentration of the whole blood and plasma was measured. Eight plasma samples at 5, 10, 15, 30, 40, 60, 70, and 90 minutes were analyzed for metabolites using an on-line system with a reverse-phase high-performance liquid chromatography linked to radioactivity and absorbance detectors connected to a PC-based integrator.[21] The level of [11C]PIB and other ^{11}C components at each sample time was calculated as a percentage of total radioactive component in each analyte, and the function of unmetabolized parent fraction in plasma was obtained from the fit of sigmoidal function for the parent fraction to the eight measurements as shown previously by Edison *et al.*[22] In their paper, it was reported that [11C]PIB was relatively rapidly metabolized; parent fraction in plasma was ~20% after 20 minutes, and 10% after 60 minutes, and that there was no significant difference between the cohorts of AD patients and age-matched control subjects.[22] A metabolite-corrected plasma curve was generated by the product of the plasma activity and nonmetabolite fraction curves as reported previously.[22]

Volumetric T1-weighted MR images were obtained with a 1.5 Tesla GE Signa scanner.

Data Analysis

Magnetic resonance images were segmented and coregistered to the summation PET images by SPM2 (Functional Imaging Laboratory, Wellcome Department of Imaging Neuroscience, University College London, London, UK). Gray matter and white matter maps were obtained from the segmented MR images and thresholded (only map value > 90% of maximum value were retained) to minimize the effect of partial volume. The eight healthy volunteers and three idiopathic AD subjects were used to predefine the three kinetic classes, and the test analysis for the Super-PIB application analysis was performed on the other seven idiopathic AD subjects and eight familial AD subjects. In these subjects, the weight of each class component was calculated for all voxels within the gray matter by equation (2), and TAC of the reference region was extracted by equation (4).

Regions of interest were manually drawn on the coregistered MR images for the cerebellum, prefrontal cortex, thalamus and pons, and ROIs for the cerebellum and prefrontal cortex were masked with the gray matter maps. The respective TACs were then extracted from the dynamic PET images.

Validation of Super-PIB Extracted Reference Region

The TACs of the Super-PIB extracted region were compared with that of the cerebellum in idiopathic AD subjects to investigate whether Super-PIB can exclude pathologic gray matter region with specific binding from

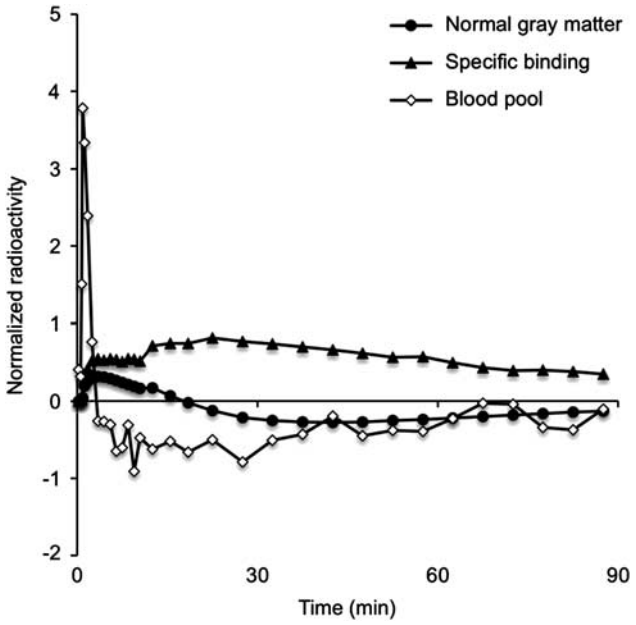

Figure 1. Normalized time–activity curve of the predefined three classes; normal gray matter, specific-binding gray matter, and blood pool.

the reference region. The total distribution volumes (V_T) were estimated for the Super-PIB extracted region and cerebellum by the Logan graphical analysis (GA) with a plasma input[23] using points after 50 minutes.

Next, the Super-PIB clustering was evaluated by investigating the distribution of Super-PIB extracted reference voxels in the cerebellum. All voxels in the cerebellum were divided into four segments according to the ratio of each kinetic class component estimated by equation (3); those with voxels regarded as a reference region (REF), those with voxels regarded as a non-reference region owing to the high specific-binding component ($R_2 \geq 0.1$ and $R_3 < 0.1$) (NREF-Binding), those regarded as a non-reference region owing to the high blood-pool component ($R_2 < 0.1$ and $R_3 \geq 0.1$) (NREF-Blood), and those regarded as a non-reference region owing to both specific binding and blood-pool components (NREF-Others). Note that the threshold values of $R_2 \geq 0.1$ or $R_3 \geq 0.1$ were determined such that R_1 value, expressed as equation (3) for kinetic class 1 ($k = 1$), would be between 0 and less than 0.9 and would be regarded as a non-reference region of non-zero to avoid spurious noise effects. The average TAC of each segment was calculated, and its V_T was estimated by GA with a plasma input. In addition, V_T values were calculated voxel-by-voxel, and the distribution of V_T values for voxels within each segment was investigated.

Comparison between Plasma Input and Reference Input Graphical Analysis

First, binding potentials ($BP_{ND} = k_3/k_4$) of the target region were estimated by the GA with a plasma input function (GA-plasma)[23] in the idiopathic AD cohort. Total distribution volumes of the target regions, i.e., the gray matter, white matter, prefrontal cortex, thalamus, and pons, and reference region, i.e., the cerebellum and the Super-PIB extracted region, were

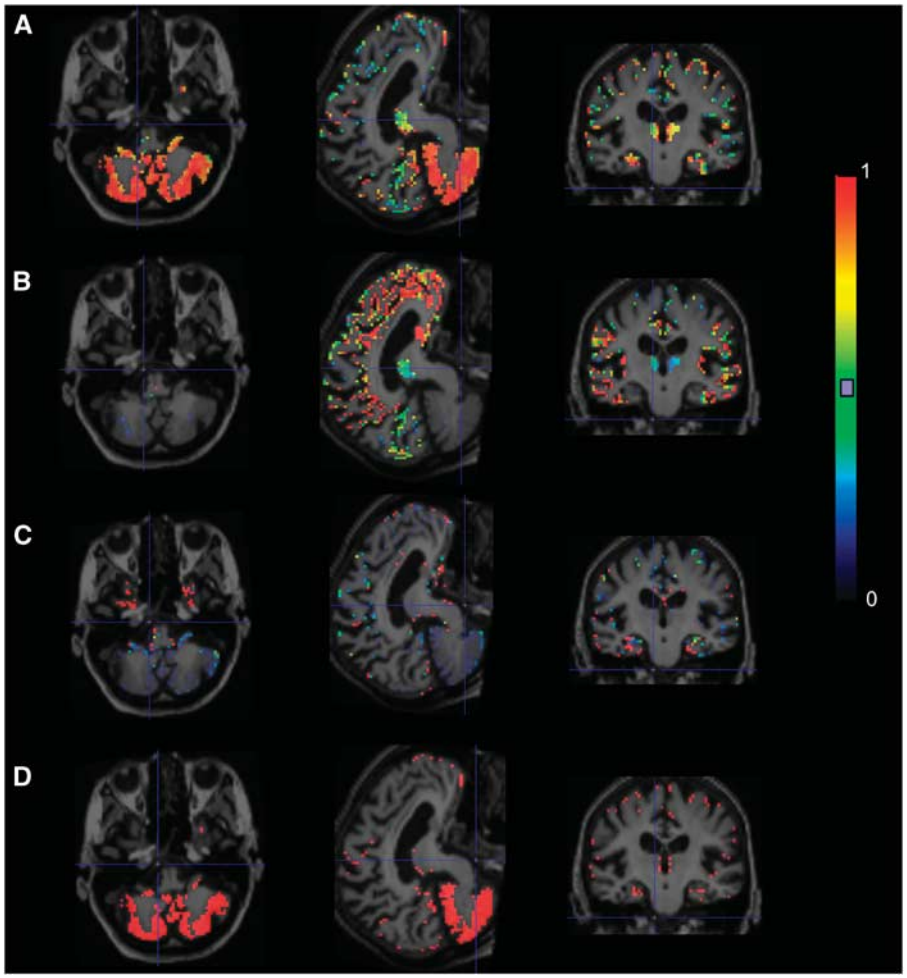

Figure 2. Maps of normal gray matter ratio (**A**), specific-binding gray matter ratio (**B**), blood-pool ratio (**C**) estimated by supervised algorithm, and extracted reference region (**D**) superimposed on magnetic resonance imaging for an idiopathic Alzheimer's disease subject.

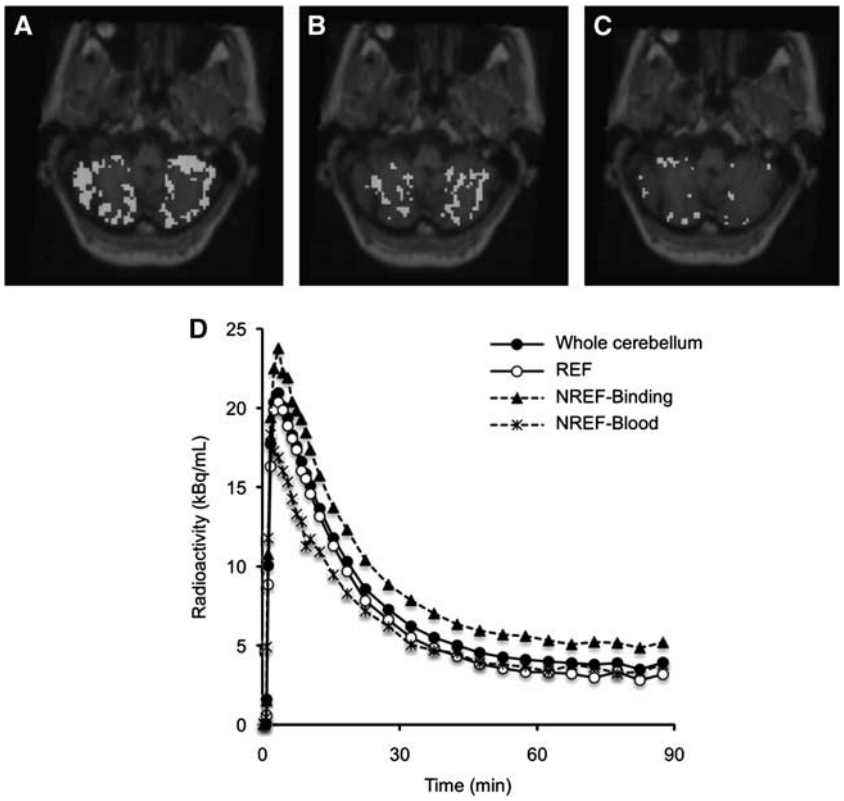

Figure 3. Example of cerebellar segmentation for the idiopathic Alzheimer's disease subject that demonstrated the higher non-reference percentage of voxels in the cerebellum; reference (**A**; REF), non-reference with high specific-binding fraction (**B**; NREF-Binding), and non-reference with high blood-pool fraction (**C**; NREF-Blood) superimposed on magnetic resonance imaging (upper), and averaged time–activity curve of the whole cerebellum and each cerebellar segment (**D**) (lower).

estimated and the BP_{ND} of target regions was calculated as;

$$BP_{ND} = \frac{V_{tg} - V_{ref}}{V_{ref}} \quad (5)$$

where V_{tg} and V_{ref} are the total distribution volume for the target and reference region, respectively, and V_{ref} is used as an estimate of the distribution volume of the free and nonspecifically bound tracer. Both the cerebellum and the Super-PIB extracted region were used as reference, and the estimated BP_{ND} were compared.

Next, BP_{ND} of the target regions were also derived from the distribution volume ratio by the GA with a reference input (GA-reference).[24] Distribution volume ratio of target–to-reference region was estimated with the Super-PIB extracted TAC as a reference input and k_2 value ($=0.149$), and BP_{ND} was calculated as;

$$BP_{ND} = V'_{tg} - 1 \quad (6)$$

where V'_{tg} is the distribution volume ratio in the target region. The estimated BP_{ND} of the target regions were compared with BP_{ND}s estimated by GA-plasma.

Binding Potential in Familial Alzheimer's Disease Patients

In the familial AD group, BP_{ND} were estimated by GA-reference with Super-PIB extracted reference region (BP_{sup}) and compared with those obtained by GA-reference with the cerebellar reference region (BP_{cer}). BP_{sup} and BP_{cer} were also estimated in the idiopathic AD group and the healthy control group. Note the kinetic classes used for the Super-PIB in eight control subjects were predefined individually from the normalized TAC of seven control subjects without the TAC of that subject itself.

Statistical Analysis

All analyses were carried out using Matlab (The Mathworks, Natick, MA, USA). Method comparison was carried out using either linear regression or Bland–Altman plots.[25] Statistical comparisons were performed using linear parametric models (Student's *t*-tests) with 0.05 as the significance level.

RESULTS

Reference Extraction by Supervised Clustering

The normalized TAC of each class defined for use in the supervised clustering is shown in Figure 1. The weight ratio of normal gray matter class (R_1) was high mainly in the cerebellum (Figure 2A), whereas the voxels of specific-binding gray matter were clustered into the cerebral cortex, such as frontal cortex, occipital cortex, and anterior cingulate (Figure 2B). The algorithm also identified the voxels with significant signal coming from the blood fraction (Figure 2C). The supervised algorithm selected as reference region a set of gray matter voxels, mostly in the cerebellum with a few in the cortices (Figure 2D).

The TACs of Super-PIB reference region were close to those of the cerebellum, though the radioactivity of Super-PIB reference region was slightly lower in later frames. The average V_T estimated by the GA-plasma for Super-PIB extracted region and the cerebellum in seven idiopathic AD subjects were 3.0 ± 0.45 and 3.3 ± 0.51, respectively. Estimated V_T of Super-PIB reference region was significantly lower than those of the cerebellum (paired *t*-test, $P < 0.05$).

Evaluation of Super-PIB Segments in the Cerebellum

Application of Super-PIB clustering in idiopathic AD patients resulted in the cerebellum being divided into segments, i.e., REF, NREF-Binding, NREF-Blood, and NREF-Others. The case where the ratio of non-reference voxels in the cerebellum was largest among seven subjects is shown in Figure 3 and related TACs are shown in Figure 3D that clearly demonstrates the tracer retention at late times for the TAC of the NREF-Binding segment. In this instance, the V_T values estimated by GA-plasma were 4.16 for the whole cerebellum (5180 voxels), 3.36 in the REF segment (2790 voxels),

Table 1. V_T estimates of each cerebellar segment in idiopathic AD patients ($n = 7$)

	Whole cerebellum	*REF*	*NREF*	*NREF-binding*	*NREF-blood*
Ratio of voxels (%)[a]	–	72 ± 12	28 ± 12	10 ± 9.5	14 ± 4.0
V_T	3.3 ± 0.51	3.0 ± 0.42	3.9 ± 0.83	4.5 ± 0.76	2.9 ± 0.56

AD, Alzheimer's disease; NREF, non-reference region; NREF-Blood, non-reference with high blood-pool fraction; NREF-Binding, non-reference region with high specific-binding fraction; REF, reference.
[a]Ratio of voxels is defined as the number of voxels belonging to each cerebellum segment divided by the number of all voxels within the cerebellum.

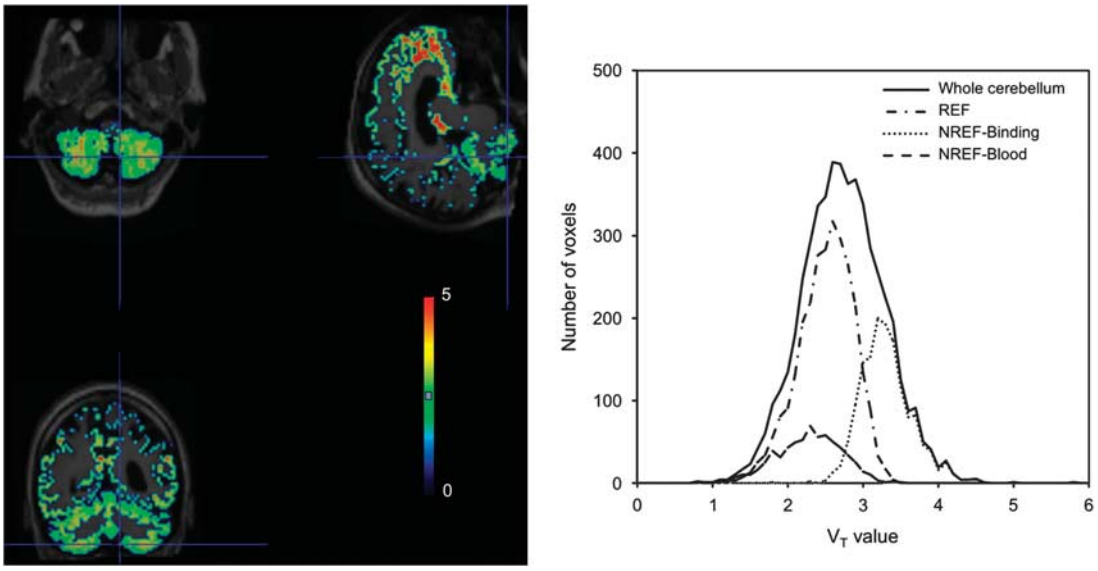

Figure 4. Parametric V_T map of the same idiopathic Alzheimer's disease subject obtained using a plasma input function (left) and histogram of V_T estimates for voxels within each cerebellar segment identified by the supervised algorithm. REF, reference; NREF-Binding, non-reference region with high specific-binding fraction; NREF-Blood, non-reference with high blood-pool fraction.

5.58 in the NREF-Binding segment (1477 voxels), and 3.27 in the NREF-Blood segment (652 voxels). This result was consistently repeated in the other six subjects. For all seven subjects, ~70% of voxels in the cerebellum belonged to the reference region segment, and V_T estimate of REF was much lower than that of NREF (Table 1).

The histograms of the V_T value from voxel-wise GA for the cerebellum of a subject are shown in Figure 4. The V_T distribution of voxels in the NREF-Binding segment was higher than that in the REF and NREF-Blood segments. In this subject, the mean value of V_T estimates of REF, NREF-Blood, and NREF-Binding were 2.5, 2.3, and 3.3, respectively.

Comparison between Plasma Input and Reference Input Graphical Analysis

In the GA-plasma, BP_{ND} of target regions estimated with V_T of Super-PIB extracted region were higher than that with V_T of the cerebellum. However, there was a good correlation between both methods (Figure 5A). In the comparison between BP_{ND} by the GA-plasma and GA-reference, there was a good correlation between both methods, though BP_{ND}s by GA-reference were underestimated (Figure 5B). The Bland–Altman plot demonstrates that underestimation is present for the high-end BP_{ND} (Figure 5C) and is the result of the known bias introduced by the GA-reference technique and not by the reference TAC itself.

Binding Potential in Familial Alzheimer's Disease Patients

In familial AD subjects, BP_{ND} of the prefrontal cortex estimated by GA-reference with Super-PIB reference was (0.83 ± 0.36 (mean ± s.d.)), clearly higher than those with the cerebellar reference (0.63 ± 0.40 (mean ± s.d.)) (Figure 6), and these differences were statistically significant (paired *t*-test, $P < 0.01$). Percentage wise, the difference between BP_{sup} and BP_{cer} was (−1.8% to 75% (mean ± s.d. 30 ± 25)) in the familial AD group compared with −6.2% to 25% (mean ± s.d.) 14 ± 11)) in the idiopathic AD group.

Note that the use of the novel reference methodology results in an increase of the BP_{ND} in the target regions also in controls; these BP_{ND} values are also greater than 0 (although no amyloid is expected in this cohort). This result is consistent with the demonstrated binding of [11C]PIB to myelin in the healthy brain.[11] The novel reference is selected on pure gray matter voxels and this minimizes partial volume effects from white to gray matter and reduces the baseline signal in the reference. This then results in the BP_{ND} of the target regions being higher and also greater than 0 given the specific binding of the tracer to the myelin protein content of the target white matter.

DISCUSSION

The aim of this work was to develop and validate an automatic extraction algorithm for the accurate identification of a reference region in dynamic [11C]PIB studies.

The methodology is based on the principle that the kinetics of the gray matter voxel can be explained as a linear mixture of healthy gray matter plus gray matter with specific binding and a blood volume component. These classes can be readily identified given the negligible presence of specific binding due to amyloid in normal volunteers and, in contrast, the widespread and intense specific binding in the cortical regions of AD patients. Therefore, it

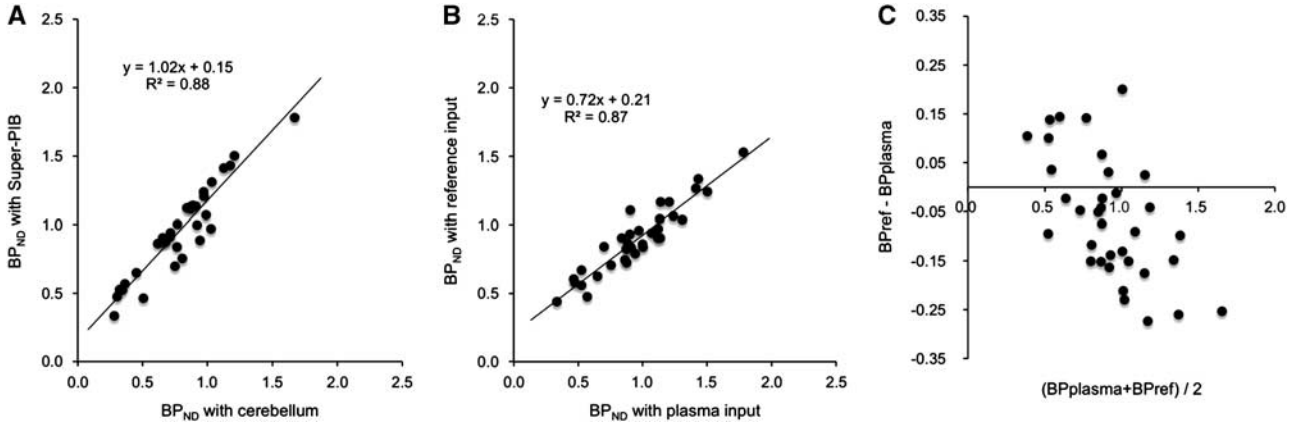

Figure 5. Relationship of binding potential (BP_{ND}) estimates between the plasma input graphical analysis using the supervised clustering extracted region and using the cerebellum as a reference region (**A**), relationship of BP_{ND} estimates between the plasma input graphical analysis and reference input graphical analysis using the supervised clustering extracted reference region (**B**), and Bland–Altman plots between BP_{ND} estimates with the plasma input and the supervised clustering extracted reference input (**C**).

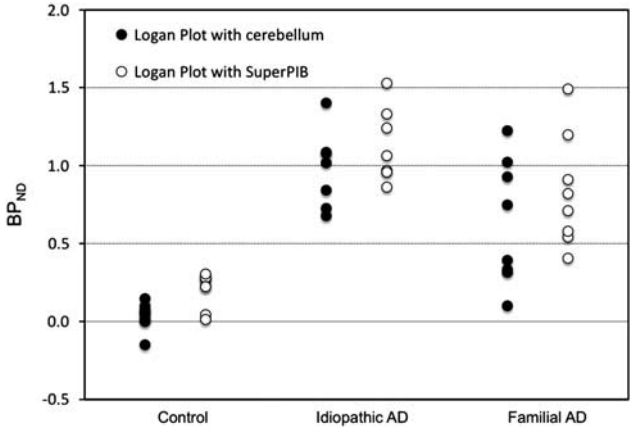

Figure 6. Binding potential (BP_{ND}) values of prefrontal cortex estimated by the reference input graphical analysis with cerebellum or supervised clustering extracted region as a reference for controls, idiopathic Alzheimer's disease (AD), and familial AD subjects.

is easy to obtain the typical kinetic pattern of a normal gray matter and a region with amyloid deposition. We acknowledge that the empirical definition of gray matter in control subjects as the tissue reference for our methodology may introduce a slight bias. A percentage of normal subjects (~30%) does seem to show low but significant amount of specific binding in gray matter regions (but not globally). However, the fact that our reference tissue was averaged on all gray matter and on all normal subjects (who, in our data set, did not seem to show any remarkable binding) renders the expected bias negligible. Differently from previous work with [11C]-(R)-PK11195,[13] we have excluded the use of normal white matter as a kinetic class given the unspecific accumulation of [11C]PIB in myelin.

Results in an idiopathic AD cohort confirmed the ability of the technology to recover a set of reference voxels, mostly cerebellar, that was away from areas of tracer accumulation as well as from areas close to or including large venous pools. Note that the inclusion of voxels with large contamination from the blood volume may introduce biases as well. In addition, in a familial AD cohort, the Super-PIB methodology demonstrated higher BP_{ND} values in target regions compared with those obtained with the cerebellar reference input. In a familial AD patient, the possibility of presence of non-neuritic amyloid plaques in the cerebellum was demonstrated,[26] and in previous PET studies with [11C]PIB, the retention of radioactivity did occur in the cerebellum, although there was considerable variability between subjects.[7] The magnitude of the BP_{ND} increase brought by the Super-PIB reference region was larger than the one in the idiopathic AD cohort, confirming that the cerebellar binding had been efficiently filtered from the reference voxels.

The novel reference methodology, by selecting highly homogeneous gray matter voxels, avoids the spillover of specific-binding signal from white matter where [11C]PIB is bound to myelin. This results in the BP_{ND} of cortical regions to be higher than the one quantified using a whole cerebellar reference. The fact that BP_{ND} in control regions is greater than 0 also confirms the previously demonstrated use of [11C]PIB as a potential marker of myelin in neurodegenerative disorders such as multiple sclerosis.[11]

The accuracy of the quantification achieved was confirmed by the good match between plasma and reference quantification. The underestimation of BP_{ND} in the GA with reference input was observed when BP_{ND} was larger and is the same bias observed in previous reports using the cerebellum as a reference input, which is due to the graphical estimation methodology.[5]

As the previous application of supervised clustering has demonstrated,[14] the technique can be robustly applied across centers and scanners as long as injecting protocols, scanner resolution properties, and reconstruction parameters are similar. However, in case kinetic classes will have to be re-defined, as explained in the previous paragraph, in the case of [11C]PIB this is quite straightforward. Clinical use of the methodology may require the redefinition of the kinetic classes if scanner resolution and/or reconstruction parameters differ. In particular, given the experience with a similar methodology for [11C]-(R)-PK11195 studies,[14] we identified significant changes in the class profiles when moving to 5 to 2 mm resolution and from filtered back-projection to iterative reconstruction approaches.

In summary, the supervised clustering method automatically detects a reliable reference region in [11C]PIB PET dynamic studies, it is a useful and practical tool for the accurate quantification of the specific binding of the radiotracer and is a methodology of general applicability.

DISCLOSURE/CONFLICT OF INTEREST

The authors declare no conflict of interest.

ACKNOWLEDGEMENTS

FET was supported by the 'PET Methodology Programme Grant' from the Medical Research Council UK (G1100809/1).

REFERENCES

1 Klunk WE, Engler H, Nordberg A, Wang Y, Blomqvist G, Holt DP *et al.* Imaging brain amyloid in Alzheimer's disease with Pittsburgh compound-B. *Ann Neurol* 2004; **55**: 306–319.
2 Rowe C, Ng S, Ackermann U, Gong S, Pike K, Savage G *et al.* Imaging beta-amyloid burden in aging and dementia. *Neurology* 2007; **68**: 1718–1725.
3 Nordberg A. Amyloid imaging in Alzheimer's disease. *Curr Opin Neurol* 2007; **20**: 398–402.
4 Price JC, Klunk WE, Lopresti BJ, Lu X, Hoge JA, Ziolko SK *et al.* Kinetic modeling of amyloid binding in humans using PET imaging and Pittsburgh compound-B. *J Cereb Blood Flow Metab* 2005; **25**: 1528–1547.
5 Lopresti BJ, Klunk WE, Mathis Ca, Hoge Ja, Ziolko SK, Lu X *et al.* Simplified quantification of Pittsburgh compound B amyloid imaging PET studies: a comparative analysis. *J Nucl Med* 2005; **46**: 1959–1972.
6 Klunk WE, Price JC, Mathis CA, Tsopelas ND, Lopresti BJ, Ziolko SK *et al.* Amyloid deposition begins in the striatum of presenilin-1 mutation carriers from two unrelated pedigrees. *J Neurosci* 2007; **27**: 6174–6184.
7 Knight WD, Okello AA, Ryan NS, Turkheimer FE, Rodríguez Martinez de Llano S, Edison P *et al.* Carbon-11-Pittsburgh compound B positron emission tomography imaging of amyloid deposition in presenilin 1 mutation carriers. *Brain* 2011; **134**: 293–300.
8 Edison P, Hinz R, Ramlackhansingh A, Thomas J, Gelosa G, Archer HA *et al.* Can target-to-pons ratio be used as a reliable method for the analysis of [11C]PIB brain scans? *NeuroImage* 2012; **60**: 1716–1723.
9 Mormino EC, Brandel MG, Madison CM, Rabinovici GD, Marks S, Baker SL *et al.* Not quite PIB-positive, not quite PIB-negative: slight PIB elevations in elderly normal control subjects are biologically relevant. *NeuroImage* 2012; **59**: 1152–1160.
10 Ikonomovic MD, Abrahamson EE, Price JC, Hamilton RL, Mathis CA, Paljug WR *et al.* Early AD pathology in a [C-11]PiB-negative case: a PiB-amyloid imaging, biochemical, and immunohistochemical study. *Acta neuropathologica* 2012; **123**: 433–447.
11 Stankoff B, Freeman L, Aigrot M-S, Chardain A, Dollé F, Williams A *et al.* Imaging central nervous system myelin by positron emission tomography in multiple sclerosis using [methyl-11C]-2-(4'-methylaminophenyl)-6-hydroxybenzothiazole. *Ann Neurol* 2011; **69**: 673–680.
12 Gunn R, Lammertsma A, Cunningham V. Parametric imaging of ligand-receptor interactions using a reference tissue model and cluster analysis. In: Carson R, Daube-Witherspoon M, Herscovitch P (eds) *Quantitative functional brain imaging with positron emission tomography*. Academic Press: San Diego, CA, 1998, pp 401–406.
13 Turkheimer FE, Edison P, Pavese N, Roncaroli F, Anderson AN, Hammers A *et al.* Reference and target region modeling of [11C]-(R)-PK11195 brain studies. *J Nucl Med* 2007; **48**: 158–167.
14 Yaqub M, Berckel BNM, Van, Schuitemaker A, Hinz R, Turkheimer FE, Tomasi G *et al.* Optimization of supervised cluster analysis for extracting reference tissue input curves in (R)-[11C]PK11195 brain PET studies. *J Cereb Blood Flow Metab* 2012; **32**: 1600–1608.
15 Lawson C, Hanson B. *Solving least squares problems*. Prentice-Hall: Englewood Cliffs, NJ, 1974.
16 Mintun MA, Larossa GN, Sheline YI, Dence CS, Lee SY, Mach RH *et al.* [11C]PIB in a nondemented population: potential antecedent marker of Alzheimer disease. *Neurology* 2006; **67**: 446–452.
17 Pike KE, Savage G, Villemagne VL, Ng S, Moss SA, Maruff P *et al.* β-amyloid imaging and memory in non-demented individuals: evidence for preclinical Alzheimer's disease. *Brain* 2007; **130**: 2837–2844.
18 Aizenstein HJ, Nebes RD, Saxton JA, Price JC, Mathis CA, Tsopelas ND *et al.* Frequent amyloid deposition without significant cognitive impairment among the elderly. *Arch Neurol* 2008; **65**: 1509–1517.
19 Jack CR, Lowe VJ, Senjem ML, Weigand SD, Kemp BJ, Shiung MM *et al.* 11C PiB and structural MRI provide complementary information in imaging of Alzheimer's disease and amnestic mild cognitive impairment. *Brain* 2008; **131**: 665–680.
20 Villemagne VL, Pike KE, Darby D, Maruff P, Savage G, Ng S *et al.* Abeta deposits in older non-demented individuals with cognitive decline are indicative of preclinical Alzheimer's disease. *Neuropsychologia* 2008; **46**: 1688–1697.
21 Luthra SK, Osman S, Turton DR, Vaja V, Dowsett K, Brady F. An automated system based on solid phase extraction and HPLC for the routine determination in plasma of unchanged [11C]-L-deprenyl; [11C]diprenrophine; [11C]flumazenil; [11C] raclopride; and [11C]Sche. *J Lab Comp Radiopharm* 1993; **32**: 518–520.
22 Edison P, Brooks DJ, Turkheimer FE, Archer HA, Hinz R. Strategies for the generation of parametric images of [11C]PIB with plasma input functions considering discriminations and reproducibility. *NeuroImage* 2009; **48**: 329–338.
23 Logan J, Fowler JS, Volkow ND, Wolf AP, Dewey SL, Schlyer DJ *et al.* Graphical analysis of reversible radioligand binding from time-activity measurements applied to [N-11C-methyl]-(-)-cocaine PET studies in human subjects. *J Cereb Blood Flow Metab* 1990; **10**: 740–747.
24 Logan J, Fowler JS, Volkow ND, Wang GJ, Ding YS, Alexoff DL. Distribution volume ratios without blood sampling from graphical analysis of PET data. *J Cereb Blood Flow Metab* 1996; **16**: 834–840.
25 Altman DG, Bland JM. Measurement in medicine: the analysis of method comparison studies. *Statistician* 1983; **32**: 307–317.
26 Verkkoniemi A, Kalimo H, Paetau A, Somer M, Iwatsubo T, Hardy J *et al.* Variant Alzheimer disease with spastic paraparesis: neuropathological phenotype. *J Neuropathol Exp Neurol* 2001; **60**: 483–492.